Supplementary Information (SI) for Physical Chemistry Chemical Physics.

Supporting information

Molecular insight into the dynamics at lithium-containing ionic liquid/gold electrode interface using electrochemical attenuated total reflection spectroscopies

Tomonori Kakinoki,[a] Akihito Imanishi, [a] Shinji Kondou, [a] Ichiro Tanabe, [b] and Ken-ichi Fukui *[a]

[a]Department of Materials Engineering Science, Graduate School of Engineering Science, Osaka University, 1-3 Machikaneyama, Toyonaka, Osaka 560-8531, Japan

[b]College of Science Department of Chemistry, Graduate School of Science, Rikkyo University, 3-34-1, Nishiikebukuro, Toshima, Tokyo 171-0021, Japan

*Corresponding author : fukui.ken-ichi.es@osaka-u.ac.jp

S1.1 Estimating the spectral shape of EMIM-TFSI on the Au electrode through optical transformation

We analyzed the ATR-FUV spectra using the optical transformation method described below. All the analyses were conducted using custom-built python scripts. According to a previous study,[1-3] the ATR-FUV spectra can be transferred into the optical parameters of a refractive index (n) and an extinction coefficient (κ) using the Kramers−Kronic transformation (KKT) method. KKT manipulation was conducted on the spectrum of neat EMIM-TFSI, as shown in Fig. 3(a). The refractive index of the sapphire prism was calculated from the Sellmeiyer equation using the parameters a = 2.022 and λ_0 = 74.54. The extinction coefficient is regarded as zero for the sapphire prism. Additionally, the parameter N_{inf}=1.42 (refractive index of EMIM-TFSI at infinite wavenumber[4]) was used. Thus, the ATR-FUV spectrum of neat EMIM-TFSI in Fig.3(a) was converted into the refractive index (n) and the extinction coefficient (κ) in Fig.S1. This is ideal for the basic spectrum utilized for KKT calculation, including the absorbance in the infinite wavelength range. The results in Fig. 3(a) are limited to a finite wavelength range (145−300 nm), therefore, the reliability of the obtained parameters decreases as the wavelength decreases. However, these optical parameters were sufficiently accurate to determine the spectral tendency, and a region longer than 160 nm was sufficiently reliable.

The extinction coefficients shown in Fig. S1(b), with the experimental transmission spectrum of EMIM-TFSI, were compared. Fig. S2 shows the transmission spectrum of the EMIM-TFSI thin film sandwiched by sapphire plates of thickness 0.1 mm. The results presented in Fig. S1(b) and Fig. S2 exhibit good consistency in their spectral shapes.

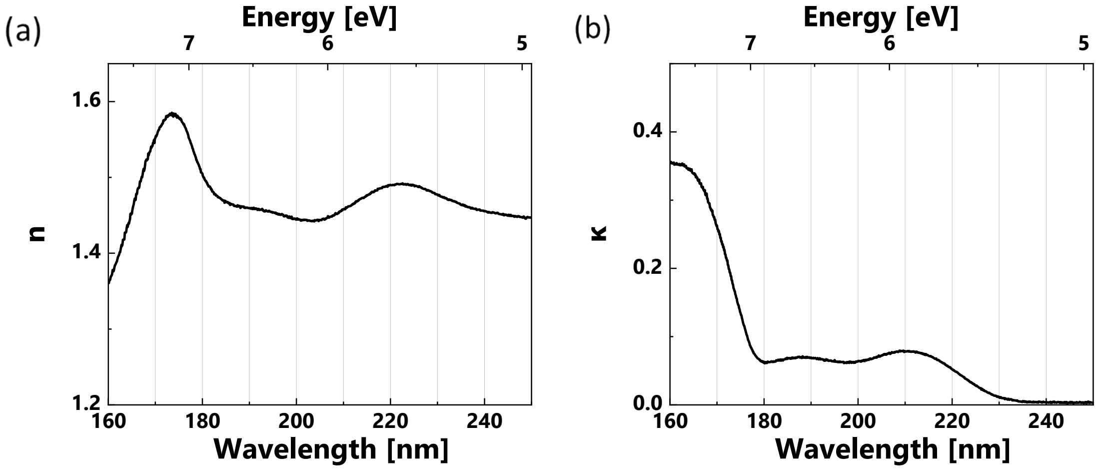

Fig. S1 (a) Refractive index and (b) extinction coefficient of EMIM-TFSI calculated using the KKT method.

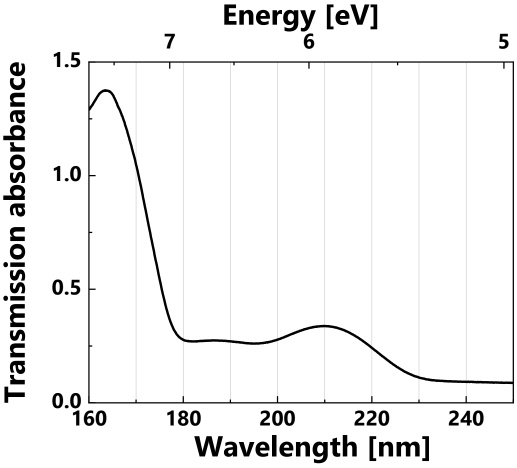

Fig. S2 Transmission spectrum of the EMIM-TFSI film sandwiched by sapphire plates of thickness 0.1 mm (reference: dry nitrogen ambient).

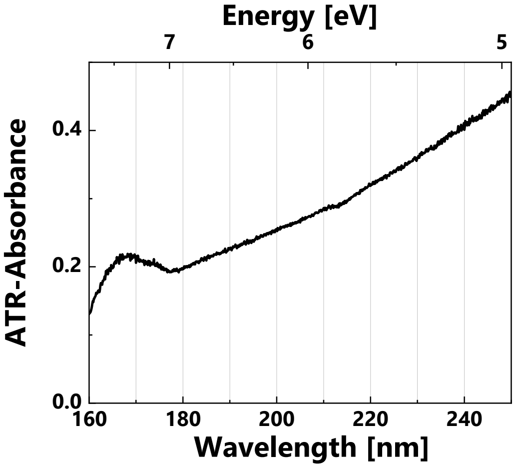

Fig. S3 Experimental ATR-FUV spectrum of a 30-nm-thick gold film on a sapphire prism (reference: bare sapphire prism).

The experimental ATR-FUV spectrum of a 30-nm-thick Au film on a sapphire prism is shown in Fig. S3. It can be confirmed that the monotonic increase in absorption in this spectral range and the small peak around 160 nm originate from the Au film.

The ATR absorbance spectra corresponding to the experimental conditions were calculated using the Fresnel equation with the optical parameters of the sapphire prism, gold film, and EMIM-TFSI obtained in Fig. S1. The calculated models included the four material layers (prism, gold film, EMIM-TFSI, and air) for the sample spectrum and three material layers (prism, gold film, and air) for the reference spectrum to divide the former. The refractive index of the sapphire prism was determined from the Sellmeiyer equation using the parameters of a = 2.022 and λ_0 = 74.54. The optical parameters of gold were obtained from a previous article[5], where the parameters were prepared by liner fitting of the measuring point. The calculation was performed for both s-polarized and p-polarized light, and the absorbance was defined as their even contribution (no polarizer was used for the experiment). The experimental ATR-FUV spectrum of EMIM-TFSI on the gold film electrode and the calculated absorbance spectra are compared in Fig. S4. They demonstrated that the essence of the absorbance spectrum could be reproduced by the calculated spectrum.

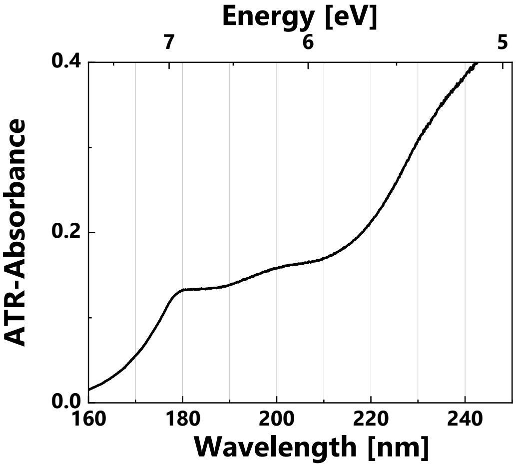

Fig. S4 Calculated absorbance spectra of EMIM-TFSI on a 14-nm-thick gold film electrode using the Fresnel equation.

S1.2 The measurement depth in the ATR spectroscopies

The penetration depth of the evanescent wave (the measurement depth in the ATR spectroscopy) is generally described by the following equation.[6]

$$d_{eva} = \frac{\lambda}{2\pi n_i n \sqrt{\left(\frac{\sin^2\theta_i}{n^2} - 1\right)}} \quad \left(n = \frac{n_t}{n_i}\right)$$

, where the λ is the wavelength of the incident light. Fig. S5 shows the estimated penetration depth of both ATR-FUV and ATR-IR spectroscopies at an ideal interface between ATR prism/IL interface. The interfacial ion alignment and movement during the electrochemical processes in our experiments should occur within the several ion layers (within a few nanometers), so the measurement depth in both methods exceeds the size of the interface. To note, the evanescent wave is decaying waves, so the electric field strength is largest at the reflection plane, and decreases exponentially away from the reflection plane to bulk electrolyte side. Thus, the information from a few layers faced to the electrode should be dominant in the experimental spectra. In electrochemical measurements, the actual measurement area is slightly shorter than in Fig. S5 because of the thin Au layer in between the ATR prism and the sample.

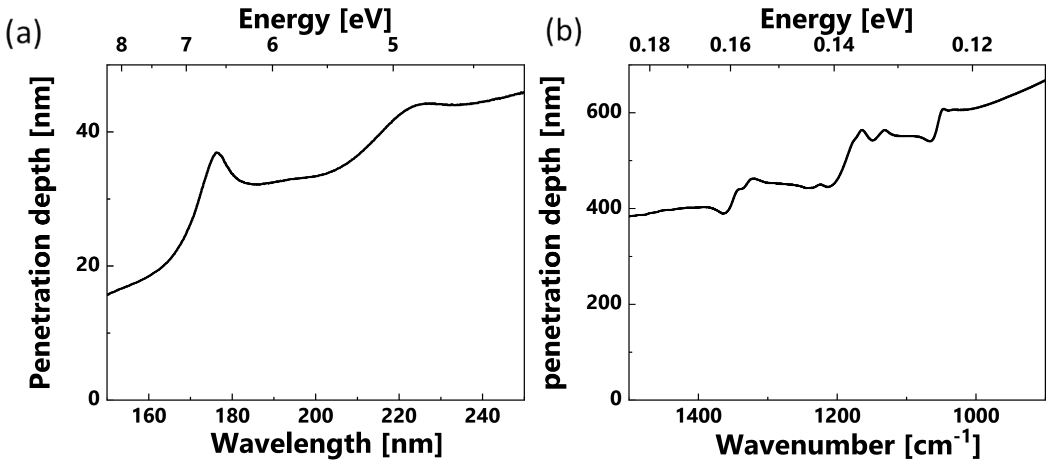

Fig. S5 The penetration depth of the evanescent wave at (a) IL / sapphire prism interface in FUV region, (b) IL / silicon prism interface in IR region, [7, 8] where the focused region including absorption from TFSI anion is shown.

In IR region, it is assumed that the excitation of surface polariton affects to the enhancement of surface spectrum. To estimate the maximum magnification rate of enhancement in the IR region, we calculated the enhancement factor (η) of the near-field light at the interface between dielectric and metal, which is solved by the following equation.[9]

$$\eta = \frac{2 \times {\varepsilon_2^{'}}^{2}}{\varepsilon_1^{0.5} \times \varepsilon_2^{''} \times (-\varepsilon_1 - \varepsilon_2^{'})^{0.5}} \quad (\varepsilon_2 = \varepsilon_2^{'} + \varepsilon_2^{''})$$

, where ε_1 and ε_2 is the dielectric function of dielectric (IL) and metal (Au).[10] In the experimental system, the maximum enhancement factor at the interface between IL and Au is solved as 200 times at 1700 cm^{-1}, where the imaginary part of the dielectric function of IL is close to 0, but the wavenumber is close to the focused position. Hence, although a thicker region is detected in the IR region relative to the size of the interface, the signal from the electrode surface is enough within the spectrum due to the enhancement effect.

The current-voltage curve obtained simultaneously with the EC-ATR-FUV spectra (shown in Fig. 4) is presented in Fig. S5. The current magnitude is sufficiently small in the entire range and has no apparent relationship with the spectral change shown in Fig. 4.

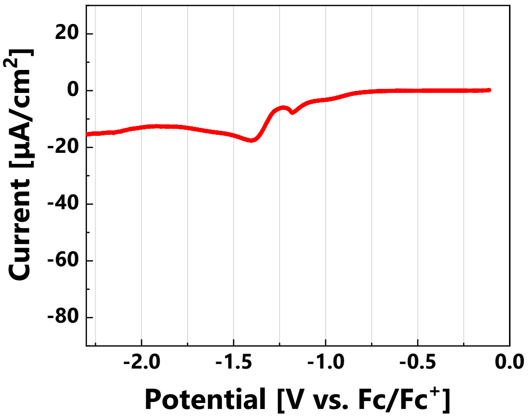

Fig. S6 Current-voltage curve measured simultaneously with ATR-FUV spectra shown in Fig.4.

References

1. A. Ikehata, N. Higashi and Y. Ozaki, *J. Chem. Phys.*, 2008, **129**, 234510.
2. A. Ikehata, T. Goto and Y. Morisawa, *Appl. Spectrosc.*, 2017, **71**, 1530.
3. M. Imai, I. Tanabe, T. Sato and K. Fukui, *Spectrochim. Acta. A*, 2022, **273**, 121040.
4. S. Seki, S. Tsuzuki, K. Hayamizu, Y. Umebayashi, N. Serizawa, K. Takei and H. Miyashiro, *J. Chem. Eng. Data*, 2012, **57**, 2211.
5. B. G. Irani, T. Huen and F. Wooten, *J. Opt. Soc. Am.*, 1971, **61**, 128.
6. Y. Ozaki, Y. Morisawa and I. Tanabe, *Chem. Soc. Rev.*, 2024, **53**, 1730.
7. D. Edwards and E. Ochoa, *Appl. Opt.*, 1980, **19**, 4130.
8. Y. Arosa, C. D. Rodríguez Fernández, E. López Lago, A. Amigo, L. M. Varela, O. Cabeza and R. de la Fuente, *Opt. Mater.*, 2017, **73**, 647.
9. G. Ford and W. Weber, *Phys. Rep.*, 1984, **113**, 195.
10. A. Rakic, A. Djurisic, J. Elazar and M. Majewski, *Appl. Opt.*, 1998, **37**, 5271.